1-1994

Neutron-Scattering Study of Librations and Intramolecular Phonons in Rb_{2.6}K_{0.4}C_{60}

D. Reznik
National Institute of Standards and Technology

W. A. Kamitakahara
National Institute of Standards and Technology

D. A. Neumann
National Institute of Standards and Technology

J. R. D. Copley
National Institute of Standards and Technology

J. E. Fischer
University of Pennsylvania

See next page for additional authors

Citation Details

Reznik, D. and Kamitakahara, W. A. and Neumann, D. A. and Copley, J. R. D. and Fischer, J. E. and Strongin, R. M. and Cichy, M. A. and Smith, A. B. (1994). Neutron-scattering study of librations and intramolecular phonons in Rb2.6K0.4C60. 49(2): 1005-1010.

Neutron-scattering study of librations and intramolecular phonons in $Rb_{2.6}K_{0.4}C_{60}$

D. Reznik, W. A. Kamitakahara, D. A. Neumann, and J. R. D. Copley
Materials Science and Engineering Laboratory, National Institute of Standards and Technology, Gaithersburg, Maryland 20899

J. E. Fischer
Laboratory for Research on the Structure of Matter and Materials Science and Engineering Department, University of Pennsylvania, Philadelphia, Pennsylvania 19104

R. M. Strongin, M. A. Cichy, and A. B. Smith III
Laboratory for Research on the Structure of Matter and Chemistry Department, University of Pennsylvania, Philadelphia, Pennsylvania 19104

(Received 7 September 1993)

We report the results of inelastic neutron-scattering measurements on $Rb_{2.6}K_{0.4}C_{60}$. Librational modes were observed as broad peaks with maxima between 4.1 and 4.7 meV, as the temperature is lowered from 300 to 12 K. As in K_3C_{60}, no change in the width or position of the librational peak was observed when the sample was cooled through the superconducting transition. Thus any coupling of the librations to electronic states is small. The magnitude of the orientational potential barrier was estimated from the librational peak frequency. A flat background observed in the low-energy inelastic-scattering spectra is ascribed to two-phonon scattering. The density of states of intramolecular modes is similar to that of previously studied M_3C_{60} compounds; modes at 53 and 66 meV in pure C_{60} are not observed in $Rb_{2.6}K_{0.4}C_{60}$.

I. INTRODUCTION

Inelastic neutron scattering has proven to be a powerful probe of the dynamics of pure C_{60} and of the alkali-metal-doped materials M_xC_{60} ($x=3$ or 6).[1-9] Neutrons couple to all normal modes of the material, and the complete spectrum of mode energies can be probed using appropriate instruments. Furthermore, the fact that thermal neutron wavelengths are comparable with interatomic distances means that information about the spatial character of the excitations can be obtained.[10] The study of lattice excitations in M_3C_{60} compounds is of particular interest, because phonons are believed to mediate superconductivity in these materials.

In M_3C_{60} compounds the fullerene molecules are on a face centered cubic (fcc) lattice and the alkali-metal ions occupy tetrahedral and octahedral intermolecular sites of the lattice,[11] contributing their valence electrons to the conduction band.[12] NMR results suggest that when more than one type of alkali metal is intercalated, the heavier ions preferentially occupy the larger octahedral sites.[13,14] X-ray diffraction results indicate that the C_{60} molecules are oriented with twofold molecular axes along the crystal axes, so that hexagons face the tetrahedral sites.[11] In this way the size of the tetrahedral sites is maximized, and the energy of the alkali-ion-C_{60} interaction is minimized. There are two orientations that satisfy this condition, and it is possible to go from one to the other, either by rotating the molecule through 90° about any one of the 001 directions or through ~44.5° about one of the 111 directions (Fig. 1). The x-ray results suggest that molecules are randomly distributed between the two types of orientations.[11]

In this paper we present the results of a detailed study of librational and intramolecular modes in $Rb_{2.6}K_{0.4}C_{60}$. We compare these results with our previous results for K_3C_{60} (Ref. 3) and in doing so we improve our understanding of the earlier data.[15]

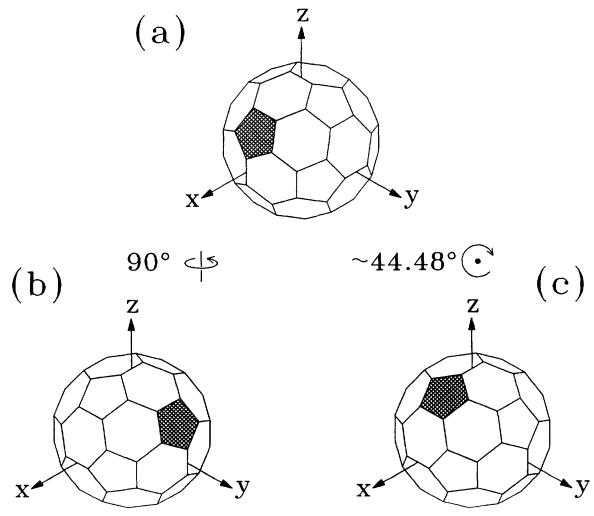

FIG. 1. The two distinct orientations of fullerenes in the Stephens model of M_3C_{60} (Ref. 11) are shown at (a) and (b). Diagrams (b) and (c) represent the same orientation which is obtained from (a) by hops about the (001) and the (111) axes, respectively. Note that $120°-\cos^{-1}(1/4)\approx 44.5°$.

II. SAMPLES AND EXPERIMENTAL DETAILS

The $Rb_{2.6}K_{0.4}C_{60}$ sample was prepared at the University of Pennsylvania from pure C_{60} powder obtained using standard procedures.[16] Synthesis of the pseudobinary alloy was achieved by diluting the saturation-doped phase Rb_6C_{60} with additional C_{60} and a small amount of K metal. The final annealing step involved heating for one week at 720 K. The superconducting transition temperature deduced from magnetic susceptibility measurements was 28 K in accordance with expectations based on the sample's stoichiometry.[17]

Two sets of neutron-scattering experiments were performed. After the initial set of measurements at the National Institute of Standards and Technology (NIST) the sample was returned to the University of Pennsylvania for unrelated experiments. The second set was performed at NIST on the same sample 6 months later. Molar ratios obtained from prompt γ ray neutron activation analysis experiments[15,18] and from an independent chemical analysis, combined with the results of diffraction experiments and a measurement of the superconducting transition temperature, led us to conclude that the stoichiometry of the sample was $Rb_{2.6}K_{0.4}C_{60}$. The H/C ratio increased from 0.5% to 1.5% between the two sets of measurements. This increase presumably occurred because of exposure to moisture. It did not affect the inelastic-scattering spectra within experimental uncertainty.

Our measurements were performed at the Neutron Beam Split-core Reactor (NBSR) at NIST. Librational modes were studied using a triple-axis spectrometer,[15] with a fixed incident neutron energy of 28 meV. The incident neutron beam was monochromated using the Cu(220) reflection, scattered neutrons were analyzed using the pyrolytic graphite (004) reflection, and collimations were 60′-40′-40′-40′. The powder sample, loaded under helium in indium-wire-sealed aluminum cylindrical cans, was placed inside a closed-cycle He refrigerator. To improve upon our earlier experimental procedure,[3] we performed a detailed measurement of the shape of the elastic resolution function over a wide energy range and for a longer counting time than in previous measurements, using a 1 cm diameter vanadium rod. The measured line shape is shown in Fig. 2. It includes two components: a strong Gaussian peak with full width at half maximum (FWHM) height of 1.03 meV, and a much broader peak whose integrated intensity is about 0.75% that of the principal peak. Since inelastic scattering is typically 2–3 orders of magnitude less intense than elastic scattering, and since the fitted line shape shown in Fig. 2 is associated with elastic scattering only, it is important to subtract the complete line shape from the raw data in order to obtain the inelastic scattering cross section. Within experimental uncertainty, the resolution function (Fig. 2) showed no dependence on the wave vector transfer Q.

The raw spectra were analyzed in several steps. Background runs were first subtracted and the spectra were corrected for changes in the scattered energy contribution to the instrumental transmission function. The fitted

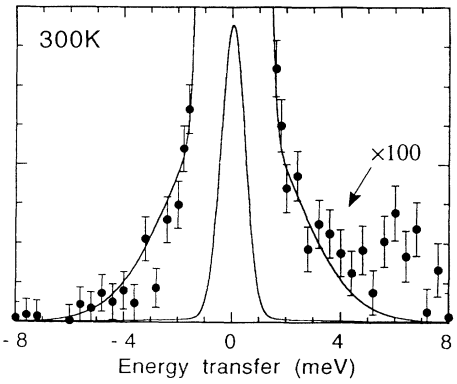

FIG. 2. A determination of the elastic resolution line shape by measurement using a vanadium rod. The weak peak at ~6 meV is probably inelastic vibrational scattering. The solid line represents a fit to the elastic component, which was a sum of two Gaussians centered at zero energy with relative integrated intensities of 1 and 0.0075, and FWHM's of 1.03 and 5.39 meV, respectively.

line shape shown in Fig. 2 was then scaled to fit the measured elastic line in the energy transfer range from -1 to 1 meV, and subtracted from the data. The result, which is proportional to the inelastic scattering function $S(Q,\omega)$, was converted to the imaginary part of the dynamical susceptibility, $\chi''(Q,\omega)$, using the fluctuation dissipation theorem:[10]

$$S(Q,\omega)=(1/\pi)[1+n(\omega)]\chi''(Q,\omega) ,$$

where $\hbar\omega$ is the neutron energy loss and $n(\omega)=(e^{\hbar\omega/k_BT}-1)^{-1}$.

For the measurements of intramolecular phonons we used a filter analyzer spectrometer. The incident neutron energy was scanned using a copper (220) crystal monochromator, and scattered neutrons with energies <1.8 meV were counted using a low-pass polycrystalline beryllium filter placed in front of the detector.[7,19] This method provides information similar to that obtained for K_3C_{60} (Ref. 4) and for Rb_3C_{60} (Ref. 5) using the TFXA time-of-flight spectrometer at the pulsed neutron source ISIS of the Rutherford-Appleton Laboratory (United Kingdom). With both methods one measures neutrons which have been scattered from high initial energies to low final energies, resulting in spectra that sample similar regions of (Q,ω) space. In our measurements the instrumental resolution varied from ~1.5 meV FWHM at 30 meV energy transfer to ~6 meV FWHM at 100 meV transfer. No corrections were applied to the data other than subtraction of container scattering and fast neutron background. The resulting spectra are directly proportional to the scattering-amplitude-weighted phonon density of states to the extent that multiphonon scattering and other sample-dependent sources of background can be neglected.[19].

III. INTERMOLECULAR MODES

The temperature dependence of the low-energy imaginary part of the dynamical susceptibility at wave-vector

transfer $Q=5.75$ Å^{-1} is shown in Fig. 3. The spectra contain two features: a broad anisotropic peak centered at 4–5 meV, which we assign to librations, and a rising background which we assign to two-phonon scattering (Sec. IV).

The librational peak maximum in $Rb_{2.6}K_{0.4}C_{60}$ occurs at ~4.1 meV at 300 K, about 0.7 meV higher than in K_3C_{60} at 300 K (Ref. 3) (presumably due to the larger size of the Rb^+ ion[15]), about 1.4 meV lower than in Rb_6C_{60} at 300 K (Ref. 3), and considerably higher than in pure C_{60} (Ref. 2). It hardens to ~4.6 meV at 12 K. The integrated intensity of the librational scattering increases with decreasing temperature, consistent with the behavior expected due to a Debye-Waller factor. Low-temperature spectra are very sensitive to errors in determining the elastic line shape, because they are less enhanced by the factor $[1+n(\omega,T)]$. The apparent upturn towards zero energy transfer, in the 12 and 35 K spectra below 2 meV, results from our inadequate determination of the elastic line shape.

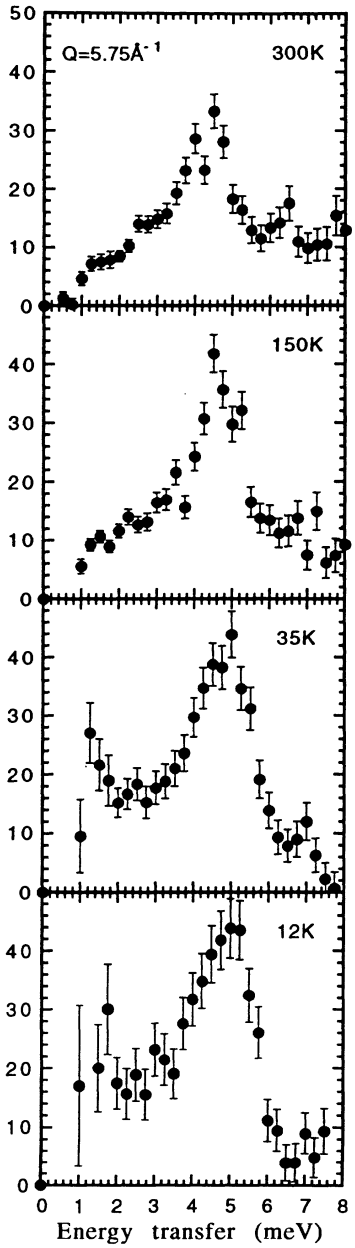

FIG. 3. Temperature dependence of the imaginary part of the dynamical susceptibility, $\chi''(Q,\omega)$, for $Rb_{2.6}K_{0.4}C_{60}$, measured by neutron scattering with momentum transfer $Q=5.75$ Å^{-1}.

At low temperatures, the librational line in $Rb_{2.6}K_{0.4}C_{60}$ and in other M_xC_{60} compounds is much broader than in pure C_{60}. This is most probably due to the more anisotropic orientational potential or to increased dispersion. As in K_3C_{60}, there is no observable narrowing of the librational peak on cooling through the superconducting transition temperature T_c (Fig. 3). Narrowing of a mode strongly coupled to conduction electrons is expected if the frequency of the mode is smaller than the superconducting gap 2Δ [which is ~13 meV for $Rb_{2.6}K_{0.4}C_{60}$ (Ref. 17)]. Thus the contribution to the peak linewidth from electron-librational coupling is small, and therefore electron-librational coupling does not play a significant role in the formation of Cooper pairs.

The spectra shown in Fig. 3 have additional intensity on the low-energy side of the librational peak. This intensity is enhanced by the factor $[1+n(\omega,T)]$ when converted to $S(Q,\omega)$, which results in the appearance of considerable intensity centered at $\omega=0$ in the corrected experimental spectra. We believe that this and the non-Gaussian tails of the resolution function are the origins of additional intensity under the elastic line observed in measurements on K_3C_{60} and Rb_6C_{60} (see Fig. 1 in Ref. 3).

The low-energy imaginary part of the dynamical susceptibility as a function of Q at 300 K is shown in Fig. 4. The solid lines represent estimates of a "background" due to two-phonon scattering (see Sec. IV). The librational peak intensity has a maximum around $Q\approx3.4$ Å^{-1}, a minimum at $Q\approx4.2$ Å^{-1}, and a sharp rise at higher Q. Figure 5 shows a comparison of the Q dependence of the integrated peak intensity with the calculated librational intensity dependence for 6.7°, 8.6°, and very large root-mean-square (rms) amplitude librations. From this comparison we estimate that the librational amplitude at 300 K is about 7°. The peak line shape does not depend strongly on Q. The principal difference among the spectra shown in Fig. 4 is the weak feature at ~2.2 meV in the low-Q spectra. If this feature is real, it may be due to either acoustic modes or to larger amplitude librations which contribute at lower energies. Differences in the Q dependences of the intensities of the low- and high-energy components may be due to anisotropies in the potential. Excitations about various axes would then have different energies and amplitudes and one would expect their Q dependences to differ.

The measured librational frequencies enable us to estimate the magnitude of the orientational potential barrier depending on the assumed size of the angle between equivalent orientations.[15] We approximate the orientational potential $V(\theta)$ by

$$V(\theta)=\frac{V_b}{2}\left[1-\cos\left[\frac{2\pi\theta}{\theta_{\text{hop}}}\right]\right]$$

where V_b is the magnitude of the potential barrier and θ_{hop} is the assumed hopping angle between orientations. Approximating $V(\theta)$ near potential minima by its quadratic component (adopting the harmonic approximation) we obtain

$$V_b = \left[\frac{2J}{\hbar^2}\right] E_{\text{lib}}^2 \left[\frac{\theta_{\text{hop}}}{2\pi}\right]^2 ,$$

where J is the moment of inertia of a C_{60} molecule ($\sim 10^{-43}$ kg m^2) and E_{lib} is the experimentally measured librational energy. Substituting the measured 300 K librational peak energies (3.6 meV for K_3C_{60} and 4.1 meV for $Rb_{2.6}K_{0.4}C_{60}$), we obtain the following room-temperature values of V_b: for K_3C_{60}, $V_b \approx 520$ meV for $\theta_{\text{hop}}=44.5°$ and $V_b \approx 2050$ meV for $\theta_{\text{hop}}=90°$; for $Rb_{2.6}K_{0.4}C_{60}$, $V_b \approx 710$ meV for $\theta_{\text{hop}}=44.5°$ and $V_b \approx 2900$ meV for $\theta_{\text{hop}}=90°$. The NMR result for the magnitude of V_b in K_3C_{60} is 460 ± 60 meV,[20] which is comparable with our estimate assuming $\theta_{\text{hop}}=44.5°$. Furthermore unpublished NMR data[21] are consistent with the value of $V_b \approx 710$ meV. Thus our data strongly suggest that reorientations mostly occur via $\sim 44.5°$ jumps about 111 axes as shown in Fig. 1. This is a very reasonable conclusion since the smaller jump angle implies that any given molecule can visit all 60 equivalent orientations, whereas 90° jumps about 100 axes sample only 12 equivalent orientations. A somewhat similar situation was found in the case of pure C_{60} (Ref. 15).

The orientational structure discussed above, derived primarily from diffraction data, is not fully consistent with recent NMR results.[14,20] The authors of Ref. 20 report that their ^{13}C spectra favor a model that assumes rotational jumps through angles somewhat smaller than 44°. Furthermore ^{87}Rb NMR experiments on Rb_3C_{60} show that there may be two types of tetrahedral sites occupied by the Rb atoms in this compound.[14] These results imply that not all of the equilibrium orientations of

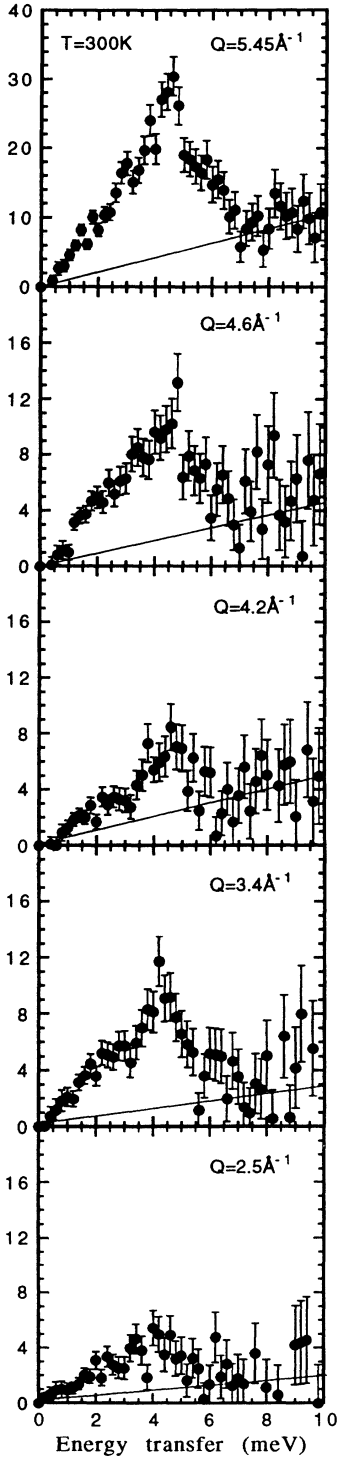

FIG. 4. Q dependence of the imaginary part of the dynamical susceptibility, $\chi''(Q,\omega)$, for $Rb_{2.6}K_{0.4}C_{60}$, measured by neutron scattering at 300 K. Solid lines represent estimates of the two-phonon contribution to the scattering.

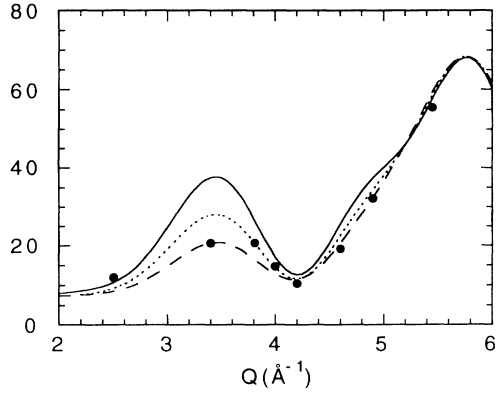

FIG. 5. Data points represent the integrated intensity of the room-temperature librational scattering. We assumed that at each Q this quantity was the difference between the integrated intensity of the spectrum (such as one of those shown in Fig. 3), between 1 and 7 meV, and the estimated two-phonon contribution. Lines are the results of theoretical calculations with a constant background added. The dashed, dotted, and solid curves represent calculations for 6.7°, 8.6°, and infinite rms amplitude librations respectively. The integrated intensities were obtained by adding up the corrected counts for the individual data points resulting in error bars smaller than the size of the symbols.

the fullerenes are included in the two-orientation model. Further investigations are necessary to better understand their results.

IV. TWO-PHONON BACKGROUND

Several of the inelastic spectra in Figs. 3 and 4 show evidence of a linearly increasing background in addition to the librational peak. The background intensity is proportional to Q^4 (see Fig. 6), and it increases with increasing T. These observations suggest that the imaginary part of the response function includes a contribution from two-phonon scattering given by[22]

$$\chi_2''(\omega,T)=\frac{1}{n(\omega)+1}e^{-2W}\frac{1}{2}\left[\frac{Q^2}{8\pi^2 m}\right]^2 \times\int_{-\infty}^{\infty}d\omega_1 f(\omega_1)f(-\omega-\omega_1)\ ,$$

where $f(\omega)=g(\omega)n(\omega)/\omega$, $g(\omega)$ is the one-phonon density of states, and e^{-2W} is a Debye-Waller factor.

$\chi_2''(\omega,T)$ is proportional to ω in the energy range of Figs. 3 and 4 if it is dominated by contributions from linearly dispersing phonon branches. Difference scattering between optical branches can also produce peaks in the low-energy spectra. Since the energies of most optical phonons are such that $\hbar\omega > k_B T$ for all temperatures at which the measurements were performed, $n(\omega)$ is small for these processes, and we believe the contribution to low-energy two-phonon scattering from the optical phonons is negligible.

Solid lines in Fig. 4 represent our estimates of the two-phonon background underneath the librational peaks at different Q. The two-phonon scattering is observed in the spectra of all C_{60} compounds measured previously, as a flat background in the raw data and a linear background in $\chi''(\omega,T)$ (Ref. 3).

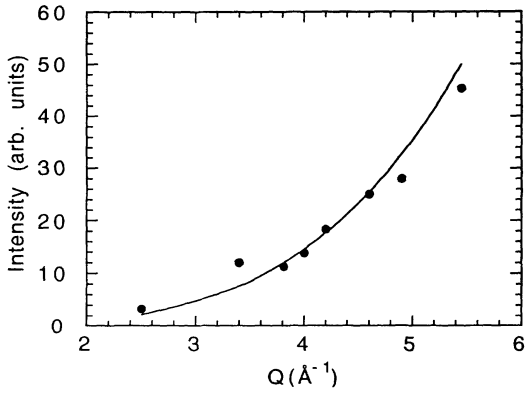

FIG. 6. Data points represent the integrated intensity of the spectra in Fig. 4 between 7 and 10 meV. The solid line is proportional to Q^4. As in Fig. 5, the error bars are smaller than the data points.

V. INTRAMOLECULAR MODES

Intramolecular vibrational modes of C_{60} molecules can also be measured by neutron scattering.[23] Experiments on M_xC_{60} compounds have already been reported, indicating that many if not all modes are broadened relative to pure C_{60}.[4,5] The systematics of the broadening, with regard to the type and frequency of the modes, is not at all clear. Figure 7 shows a comparison of spectra measured for C_{60} and for $Rb_{2.6}K_{0.4}C_{60}$ using the filter analyzer method. The smaller peak signal-to-noise ratio for the $Rb_{2.6}K_{0.4}C_{60}$ spectrum is mainly because of the smaller sample size but also because most of the peaks are significantly broadened. In the energy range of the measurement, from 30 to 100 meV, what is most noteworthy is that peaks at 53 and 66 meV in the C_{60} spectrum, Fig. 7(a), are not apparent in the spectrum for $Rb_{2.6}K_{0.4}C_{60}$, Fig. 7(b), presumably because the relevant modes have become very strongly broadened. The 53 meV peak derives from a Raman-active H_g mode, while the 66 meV peak represents a combination of an infrared-active T_{1u} mode and an optically silent H_u mode. The other peaks have also become noticeably broadened relative to C_{60}, but the broadening cannot be ascribed to a simple dependence on energy or symmetry assignments. The neutron measurements are sensitive to all modes, with associated intensities in the scattered-neutron spectrum primarily determined by mode degeneracies. The spectrum in Fig. 7(b) is similar to those previously reported for K_3C_{60} (Ref. 4) and for Rb_3C_{60} (Ref. 5). While it is tempting to ascribe the changes from C_{60} to M_3C_{60} to the interaction of conduction electrons with the vibrational modes, one should note that the intramolecular vibrational spectrum of Rb_6C_{60} (Ref. 24) also shows major differences from both C_{60} and M_3C_{60}

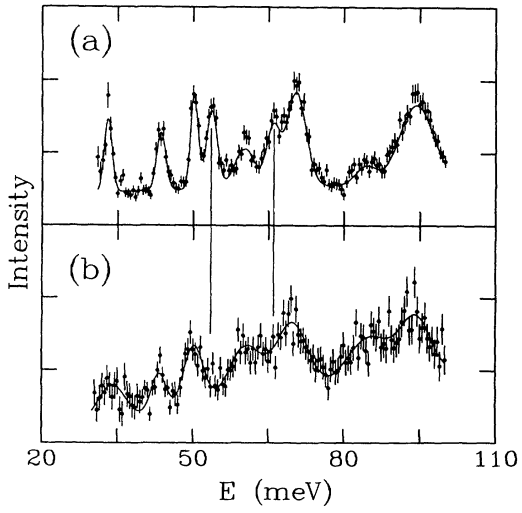

FIG. 7. (a) Intramolecular vibrational spectrum observed for C_{60}, and (b) a similar spectrum for $Rb_{2.6}K_{0.4}C_{60}$. The vertical lines at 53 and 66 meV indicate peaks in (a) which have apparently disappeared in (b).

compounds. Since Rb_6C_{60} is an insulator, the latter differences can only be ascribed to factors other than the electron-phonon interaction.

VI. CONCLUSIONS

We have measured inelastic neutron-scattering spectra for a powder sample of $Rb_{2.6}K_{0.4}C_{60}$. The librational scattering shows a broad peak centered at ~ 4.1 meV at room temperature, shifting to slightly higher energy at low temperatures. We conclude that coupling to the conduction electrons does not contribute significantly to the librational self-energy, because no change in linewidth is observed at the superconducting transition temperature. Bose factor enhancement of the low-energy tail of the spectrum results in the appearance of a broad peak centered at zero energy in the raw spectra. The magnitude of the potential barrier between degenerate orientations of the C_{60} molecules was estimated from the librational peak energies to be ~ 520 meV for K_3C_{60} and ~ 710 meV for $Rb_{2.6}K_{0.4}C_{60}$ at 300 K. The background under the librational peak is ascribed to two-phonon scattering. As with previously reported experiments we observe substantial broadening of intramolecular phonons in $Rb_{2.6}K_{0.4}C_{60}$ as compared with pure C_{60}.

ACKNOWLEDGMENTS

D.R. would like to thank the National Research Council for financial support. The authors thank R. Paul and R. Lindstrom for the prompt gamma activation measurements and R. Tycko for communicating unpublished results. The work at Penn was supported by the National Science Foundation MRL Program under Grant No. DMR91-2066 and by the Department of Energy under Grants No. DE-FC02-86ER45254 and No. DE-FG05-90ER75596.

[1]D. A. Neumann, J. R. D. Copley, R. L. Cappelletti, W. A. Kamitakahara, R. M. Lindstrom, K. M. Creegan, D. M. Cox, W. J. Romanow, N. Coustel, J. P. McCauley, Jr., N. C. Maliszewskyj, J. E. Fischer, and A. B. Smith III, Phys. Rev. Lett. **67**, 3808 (1991).

[2]D. A. Neumann, J. R. D. Copley, W. A. Kamitakahara, J. J. Rush, R. L. Cappelletti, N. Coustel, J. E. Fischer, J. P. McCauley, Jr., A. B. Smith III, K. M. Creegan, and D. M. Cox, J. Chem. Phys. **96**, 8631 (1992).

[3]C. Christides, D. A. Neumann, K. Prassides, J. R. D. Copley, J. J. Rush, M. J. Rosseinsky, D. W. Murphy, and R. C. Haddon, Phys. Rev. B **46**, 12 088 (1992).

[4]K. Prassides, J. Tomkinson, C. Christides, M. J. Rosseinsky, D. W. Murphy, and R. C. Haddon, Nature **354**, 462 (1991).

[5]J. W. White, G. Lindsell, L. Pang, A. Palmisano, D. S. Sivia, and J. Tomkinson, Chem. Phys. Lett. **191**, 92 (1992).

[6]F. Gompf, B. Renker, H. Schober, P. Adelman, and R. Heid (unpublished); B. Renker, F. Gompf, R. Heid, P. Adelman, A. Heiming, W. Reichardt, G. Roth, H. Schober, and H. Rietschel, Z. Phys. B **90**, 325 (1993).

[7]J. R. D. Copley, D. A. Neumann, R. L. Cappelletti, and W. A. Kamitakahara, J. Phys. Chem. Solids **53**, 1353 (1992).

[8]L. Pintchovius, B. Renker, F. Gompf, R. Heid, S. L. Chaplot, M. Haluska, and H. Kuzmany, Phys. Rev. Lett. **69**, 2662 (1992).

[9]C. Coulombeau, H. Jobic, P. Bernier, C. Fabre, D. Shcütz, and A. Rassat, J. Phys. Chem. **96**, 22 (1992).

[10]M. Bée, *Quasielastic Neutron Scattering* (Hilger, Bristol, 1988).

[11]P. W. Stephens, L. Mihaly, P. L. Lee, R. L. Whetten, S-M. Huang, R. Kaner, F. Deiderich, and K. Holczer, Nature **351**, 632 (1991); P. W. Stephens, L. Mihaly, J. B. Wiley, S-M. Huang, R. Kaner, F. Deiderich, R. L. Whetten, and K. Holczer, Phys. Rev. B **45**, 543 (1991).

[12]J. H. Weaver, J. Phys. Chem. Solids **53**, 1433 (1992).

[13]K. Migoguchi, Y. Maniwa, and K. Kume, Mat. Sci. Eng. **B19**, 146 (1993).

[14]R. E. Walstedt, D. W. Murphy, and M. Rosseinsky, Nature **362**, 611 (1993).

[15]D. A. Neumann, J. R. D. Copley, D. Reznik, W. A. Kamitakahara, J. J. Rush, R. L. Paul, and R. M. Lindstrom, J. Phys. Chem. Solids (to be published).

[16]J. P. McCauley, Jr., Q. Zhu, N. Coustel, O. Zhou, G. Vaughan, S. H. J. Idziak, J. E. Fischer, S. W. Tozer, D. M. Groski, N. Bykovetz, C. L. Lin, A. R. McGhie, B. H. Allen, W. J. Romanow, A. M. Denenstein, and A. B. Smith III, J. Am. Chem. Soc. **113**, 8537 (1991).

[17]Z. Zhang, C-C. Chen, and C. M. Lieber, Science **254**, 1619 (1991).

[18]M. P. Failey, D. L. Anderson, W. H. Zoller, G. E. Gordon, and R. M. Lindstrom, Anal. Chem. **51**, 2209 (1979).

[19]A. D. B. Woods, B. N. Brockhouse, M. Sakamoto, and R. N. Sinclair, in *Inelastic Scattering of Neutrons in Solids and Liquids* (IAEA, Vienna, 1961), p. 487.

[20]S. E. Barrett and R. Tycko, Phys. Rev. Lett. **69**, 3754 (1992).

[21]R. Tycko (private communication).

[22]H. Seong and S. D. Mahanti (unpublished).

[23]R. L. Cappelletti, J. R. D. Copley, W. A. Kamitakahara, Fang Li, J. S. Lannin, and D. Ramage, Phys. Rev. Lett. **66**, 3261 (1991).

[24]K. Prassides, C. Christides, M. J. Rosseinsky, J. Tomkinson, D. W. Murphy, and R. C. Haddon, Europhys. Lett. **19**, 629 (1992).